Mutagenic and Enzymological Studies of the Hydratase and Isomerase Activities of 2-Enoyl-CoA Hydratase-1†

Tiila-Riikka Kiema,‡ Christian K. Engel,§ Werner Schmitz,|| Sirpa A. Filppula,‡ Rik K. Wierenga,‡,§ and J. Kalervo Hiltunen*,‡

Biocenter Oulu and Department of Biochemistry, University of Oulu, FIN-90570 Oulu, Finland, European Molecular Biology Laboratory, Postfach 102209, D-69012 Heidelberg, Germany, and Theodor-Boveri-Institut für Biowissenschaften, Am Hubland, D-97074 Würzburg, Germany

Received July 9, 1998; Revised Manuscript Received December 10, 1998

ABSTRACT: Structural and enzymological studies have shown the importance of Glu144 and Glu164 for the catalysis by 2-enoyl-CoA hydratase-1 (crotonase). Here we report about the enzymological properties of the Glu144Ala and Glu164Ala variants of rat mitochondrial 2-enoyl-CoA hydratase-1. Size-exclusion chromatography and CD spectroscopy showed that the wild-type protein and mutants have similar oligomerization states and folding. The k_{cat} values of the active site mutants Glu144Ala and Glu164Ala were decreased about 2000-fold, but the K_m values were unchanged. For study of the potential intrinsic Δ^3-Δ^2-enoyl-CoA isomerase activity of mECH-1, a new assay using 2-enoyl-CoA hydratase-2 and (*R*)-3-hydroxyacyl-CoA dehydrogenase as auxiliary enzymes was introduced. It was demonstrated that rat wild-type mECH-1 is also capable of catalyzing isomerization with the activity ratio (isomerization/hydration) of 1/5000. The k_{cat} values of isomerization in Glu144Ala and Glu164Ala were decreased 10-fold and 1000-fold, respectively. The data are in line with the proposal that Glu164 acts as a protic amino acid residue for both the hydration and the isomerization reaction. The structural factors favoring the hydratase over the isomerase reaction have been addressed by investigating the enzymological properties of the Gln162Ala, Gln162Met, and Gln162Leu variants. The Gln162 side chain is hydrogen bonded to the Glu164 side chain; nevertheless, these mutants have enzymatic properties similar to that of the wild type, indicating that catalytic function of the Glu164 side chain in the hydratase and isomerase reaction does not depend on the interactions with the Gln162 side chain.

Mitochondrial 2-enoyl-CoA hydratase-1 (crotonase) (mECH-1)[1] (EC 4.2.1.17), an enzyme of the fatty acid β-oxidation cycle in this cellular compartment, catalyzes the reversible hydration of *trans*-2-enoyl-CoA to (*S*)-3-hydroxyacyl-CoA (*1*−*3*). mECH-1 is a member of the protein family with the low-homology hydratase/isomerase sequence pattern and with diversified physiological functions; e.g., it includes enzymes such as Δ^3-Δ^2-enoyl-CoA isomerase (EC 5.3.3.8) (*4*, *5*), 4-chlorobenzoyl-CoA dehalogenase (*6*, *7*), the N-terminal domain of β-oxidation multifunctional enzymes (MFE) type 1 (*8*−*10*), $\Delta^{3,5}$-$\Delta^{2,4}$-dienoyl-CoA isomerase (*11*), naphthoate synthase (*12*), and carnitine racemase (*13*).

Members of the hydratase/isomerase family in the fatty acid β-oxidation have been described to catalyze hydratase or isomerase reactions (Figure 1). These reactions are closely related, and they include a proton transfer at the α-carbon of the substrate. In mammalian mitochondria the reactions

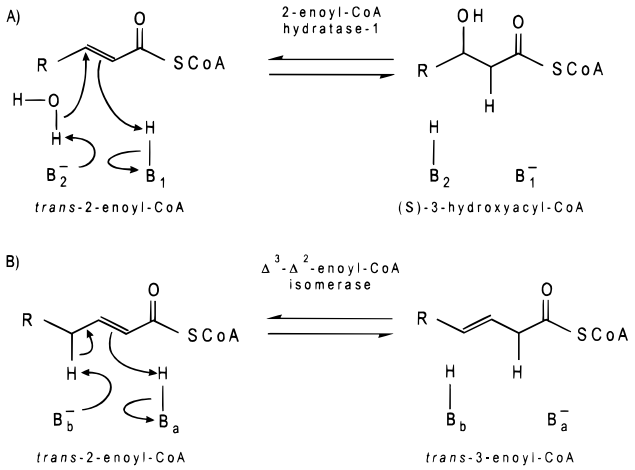

FIGURE 1: Reactions carried out by 2-enoyl-CoA hydratase-1 (A) and Δ^3-Δ^2-enoyl-CoA isomerase (B). Hydratase catalyzes the syn addition of water to the C2−C3 double bond (*16*) producing (*S*)-3-hydroxyacyl-CoA; therefore, both catalytic groups are below the plane of the drawing. Multifunctional β-oxidation enzymes can catalyze both reactions. Acids H−B_1 and H−B_a are Glu164 in enoyl-CoA hydratase and its equivalent in enoyl-CoA isomerase, respectively. Base B_2^- in the case of the hydratase is Glu144, and B_b^- for the enoyl-CoA isomerase is unknown. For clarity only selected atoms are displayed.

† This work was supported by grants from the Sigrid Juselius Foundation, the Academy of Finland, the Deutscher Akademischer Austauschdienst, and the Deutsche Forschungsgemeinschaft (Grant Co 116-3/1).

* Corresponding author. Tel: +358 8 5531150. Fax: +358 8 5531141. E-mail: Kalervo.Hiltunen@oulu.fi.

‡ University of Oulu.

§ European Molecular Biology Laboratory.

|| Theodor-Boveri-Institut für Biowissenschaften.

[1] Abbreviations: CD, circular dichroism; GLC, gas−liquid chromatography; isomerase, Δ^3-Δ^2-enoyl-CoA isomerase; mECH-1, mitochondrial 2-enoyl-CoA hydratase-1; MFE, multifunctional enzyme; PDB, Brookhaven Protein Data Bank.-

10.1021/bi981646v CCC: $18.00
Published on Web 02/19/1999

are catalyzed by separate enzymes, but in peroxisomes and in bacteria both activities have been assigned to the same multifunctional polypeptide (*14*). According to sequence analysis the N-terminal domain of the MFE type 1 from rat peroxisomes (*4*) as well as from *Escherichia coli* (*15*) contains only one CoA-binding site; the active site of this domain is thought to catalyze both the isomerase and the hydratase reaction.

Detailed mechanistic studies of the hydratase reaction have shown that it follows syn stereochemistry (*16*) and is concerted (*17*). The structural data of mECH-1, amino acid sequence comparison to other hydratase/isomerase proteins, and mutagenesis data suggest that two carboxylic acid side chains participate in catalysis (*3, 18, 19*) (Figure 1A). For example, studies on the hydratase domain of the bacterial MFE have shown that the hydratase-1 activity of Glu139Gln and Glu119Gln (equivalent to Glu164 and Glu144 in hydratase-1) is decreased by a factor of 3000 and 100, respectively (*15, 19*). In addition, it has been found that the Glu164Gln variant of hydratase-1 is 100 000-fold less active than wild type (*20, 21*). In the crystal structure of mECH-1 (*3, 22*) a water molecule is bound between Glu144 and Glu164 of the unliganded active site (Figure 2). According to the proposed reaction mechanism Glu144 serves as an acceptor of the proton from a water molecule that carries out a nucleophilic attack at the β-carbon. The geometry of the active site of mECH-1 (Figure 2) shows that the γ-carboxylic group of Glu164 is closer than 4 Å to the α-carbon of the substrate which is being protonated during catalysis. The amino acid sequence alignment of the hydratase/isomerase family revealed that the glutamate corresponding to Glu144 in mECH-1 is conserved among the members catalyzing hydratase reaction but not among other members (*18, 20, 23*), whereas Glu164 is conserved in all members catalyzing either isomerization and/or hydration (Figure 3).

The structure of the Δ^3-Δ^2-enoyl-CoA isomerase has not yet been determined (*24*); therefore, the active site geometry of the isomerase is not known. From isomerase mutagenesis studies of the equivalent of Glu164, it is found that changing this glutamate to a glutamine almost completely abolished the catalytic activity (*23*). On the basis of the sequence homology between the hydratases and the isomerases it seems very likely that this glutamate activates the proton of the α-atom (base B_a^- in Figure 1B). The second protic residue (B_b, Figure 1B) of the isomerase reaction is unknown. It could, for example, be a water molecule, but it could also potentially be the side chain equivalent to Glu164 in mECH-1.

Here we report further enzymological studies of hydratase-1. First, we established that wild-type hydratase-1 has also isomerase activity and report the pH dependency of the activities. Second, we describe the hydratase and isomerase activity of the Glu144Ala and Glu164Ala variants. Third, we address the question of which factors might be important for determining the relative rates of the hydratase and isomerase reaction.

MATERIALS AND METHODS

Synthesis of Recombinant mECH-1 cDNA and Construction of the Wild-Type pETH1 Expression Vector. Total RNA from Wistar rat liver was subjected to reverse transcription with M-MuLV reverse transcriptase (Gibco-BRL Life Technologies, Gaithersburg, MD), and subsequently the cDNA coding for mECH-1 was amplified by PCR using the specific primers HydraS (5′ GGA ATT CCA TAT GGG TGC TAA CTT 3′) and HydraAS (5′ AAG GAT CCT CAG TGG TCT TTG AA 3′). The mECH-1 cDNA was subcloned into the pUC18 (pUC18ECH1) vector using the Sure Clone ligation kit (Amersham Pharmacia Biotech, Uppsala, Sweden). The *Nde*I and *Bam*HI restriction sites added in primers enabled cloning of the cDNA into the *E. coli* pET3a expression vector (Novagen, Madison, WI). All amplification reactions were performed with high fidelity *Pfu* polymerase (Stratagene, La Jolla, CA) using primers synthesized with an Applied Biosystems DNA synthesizer (Perkin-Elmer, Norwalk, CT).

Construction of the pET3aECH1(E144A) Mutant Expression Vector. The mutation Glu144 to alanine was introduced to mECH-1 by overlapping extension PCR (*25*) using the pUC18ECH1 plasmid DNA as a template. HydraS and HydraAS were used as flanking primers and E144A (5′ C TGT G**C**A CTT GCC ATG AT 3′) and reversed E144A as mutagenic primers. The final PCR product was cloned into the pUC18 vector. The resulting pUC18ECH1(E144A) vector was digested with the restriction enzymes *Nde*I and *Bam*HI (Fermentas, Vilnius, Lithuania), and the insert was cloned into the pET3a expression vector.

Construction of the Mutant Expression Vectors pET3aECH1(E164A), pET3aECH1(Q162A), pET3aECH1(Q162L), pET3aECH1(Q162M), and pET3aECH1(E144A,Q162L). A QuikChange mutagenesis kit (Stratagene) was applied for constructing the pET3aECH1(E164A), pET3aECH1(Q162A), pET3aECH1(Q162L), pET3aECH1(Q162M), and pET3aECH1(E144A,Q162L) mutant expression vectors. The pET3aECH1(E144A) expression vector was used as a template for constructing the pET3aECH1(E144A,Q162L) vector for the expression of a double mutant mECH-1; otherwise, pET3aECH1 was used as a template. The mutagenic primers (E164A, 5′ G TTT GGA CAG CCA G**C**A ATC CTC CTG GG 3′; Q162A, 5′ C CAG TTT GGA **GC**G CCA GAA ATC CTC 3′; Q162L, 5′ C CAG TTT GGA C**T**G CCA GAA ATC CTC 3′; Q162M, 5′ C CAG TTT GGA **AT**G CCA GAA ATC CTC 3′) were purified on 12% polyacrylamide gel. The constructs and mutations were confirmed by sequencing (T7 sequencing kit, Amersham Pharmacia Biotech).

Overexpression and Purification of the Wild-Type and Mutant Forms of Recombinant mECH-1. Wild-type or mutant variants of mECH-1 were expressed in *E. coli* BL21(DE3)-pLysS cells following the supplier's instructions (Novagen). The bacterial cells were isolated, suspensed in 30 mM KP_i, pH 7.2, and stored at −70 °C. After thawing (1.2 g of *E. coli* cells), DNase I (Amersham Pharmacia Biotech), RNase A (Sigma Chemicals, St. Louis, MO), lysozyme (Sigma Chemicals), β-mercaptoethanol, and $MgSO_4$ were added to final concentrations of 20 μg/mL, 2 μg/mL, 100 μg/mL, 0.5 mM, and 10 mM, respectively. After 30 min at 35 °C EDTA (3 mM final concentration) was added and the cell lysate was centrifuged (30000*g*, 45 min, 4 °C). Supernatant was applied to the anion exchanger DEAE-Sephacel (7 cm × 2.5 cm) equilibrated with 30 mM KP_i, pH 7.2. The flow-through fractions containing the recombinant mECH-1 were collected and dialyzed twice against 20× volume of 25 mM Tris-HCl, 1 mM EDTA, pH 8.5, and 0.5 mM β-mercapto-

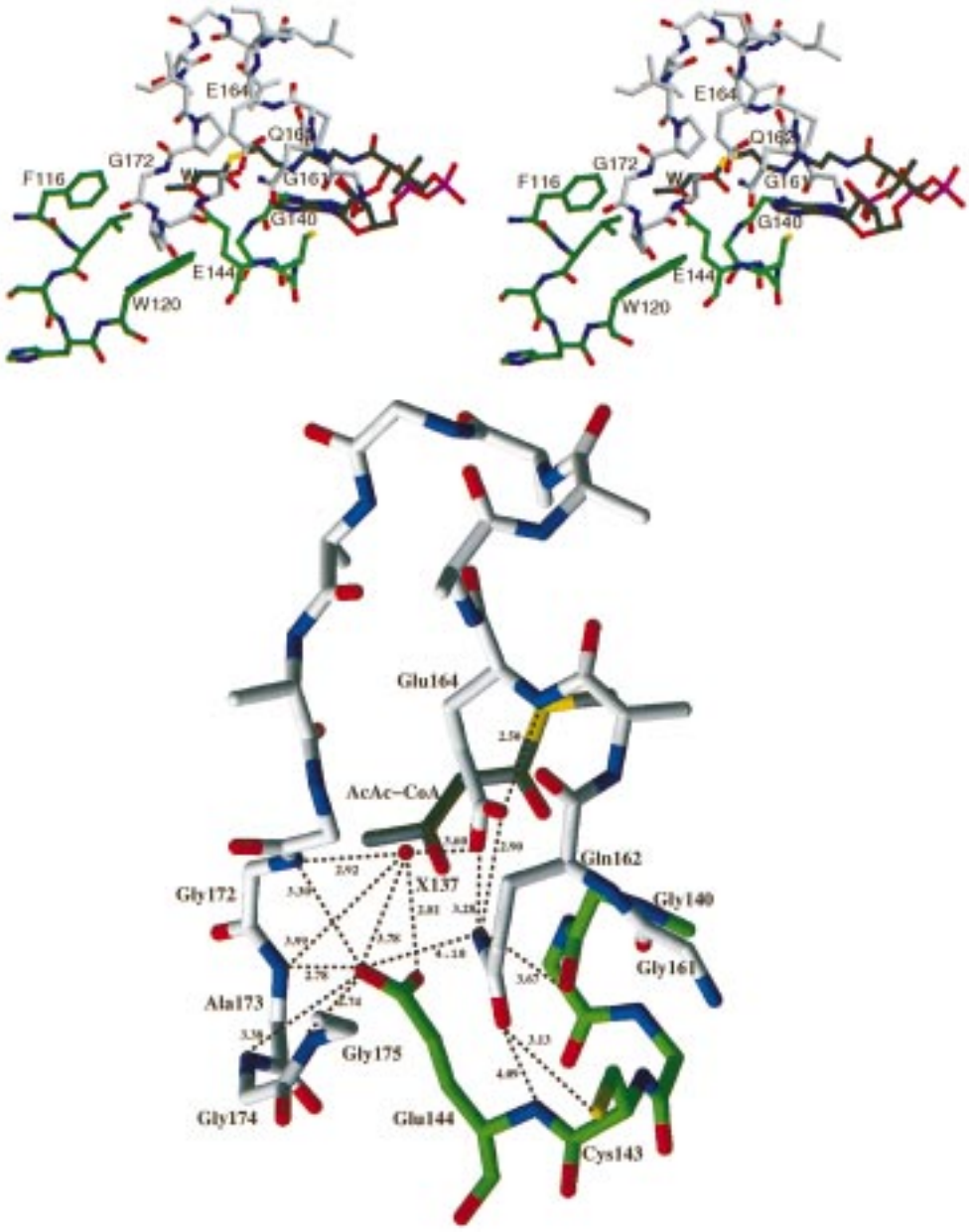

FIGURE 2: (A, top) Active site geometry. The coordinates are taken from the structure of the complex of mECH-1 with acetoacetyl-CoA (entry 1DUB of the PDB). In this complex one active site is unliganded, and in five active sites an acetoacetyl-CoA molecule is bound. The stereo picture shows the geometry of the unliganded active site, including the active site water molecule (W) believed to be prepositioned for catalysis. Also shown is a superimposed acetoacetyl-CoA molecule (dark gray carbon atoms). The following protein fragments are included in this picture: Gly140 to Glu144 (the active site helix; light green carbon atoms), Gly161 to Gly175 (including the GAGG turn Gly172−Gly175; gray carbon atoms), and Phe116 to Trp120 (the flexible loop; dark green carbon atoms). The picture was made with MOLSCRIPT (*39*) and RASTER3D (*40*). (B, bottom) Active site distances (same view as in panel A). The dotted lines show the distances of the polar atoms of the side chains of Glu144, Gln164, and the active site water X137 to other polar atoms within the active site pocket. Two polypeptide stretches at the active site are displayed. Nitrogen (blue), oxygen (red), and sulfur (yellow) atoms are colored according to atom type; the carbon atoms are in gray for the stretch Gly161 to Gly175, including the GAGG turn, and light green for Gly140 to Glu144 (part of the active site helix). For clarity some side chains have been omitted; the picture also shows the *S*-acetoacetyl moiety (carbon atoms in dark gray) of a superimposed acetoacetyl-CoA. The picture was made with ICM (*41*).

ethanol. The sample was applied to the anion exchanger Resource Q (Amersham Pharmacia Biotech, 1 mL bed volume) in equilibrium with the dialysis buffer, and the bound mECH-1 was eluted with a linear gradient of 25 mL of 0−0.25 M NaCl in the dialysis buffer. The peak fractions containing mECH-1 were pooled and applied to the Superdex 200 HR 10/30 size-exclusion column (Amersham Pharmacia Biotech) in equilibrium with 200 mM KP_i, 3 mM EDTA, and 3 mM EGTA, pH 7.2. The fractions containing mECH-1 (total: 1.5 mg of proteins) were concentrated by centrifugal ultrafiltration (Ultrafree-CL 10000 NMWL, Millipore, Bedford, MA) to 1 mL.

Circular Dichroism (CD) Spectroscopy. CD spectroscopy was carried out at 22 °C using a Jasco J710 spectropolarimeter. Absorption at 280 nm (*26*) was measured for all samples and used for fine adjustment of the protein concentration of the sample used for CD spectroscopy. The far-UV spectra (Figure 4A,C) of the proteins were measured from 195 to 250 nm in 40 mM KP_i and 3 mM EDTA, pH 7.2, with the following instrument settings: response 1 s,

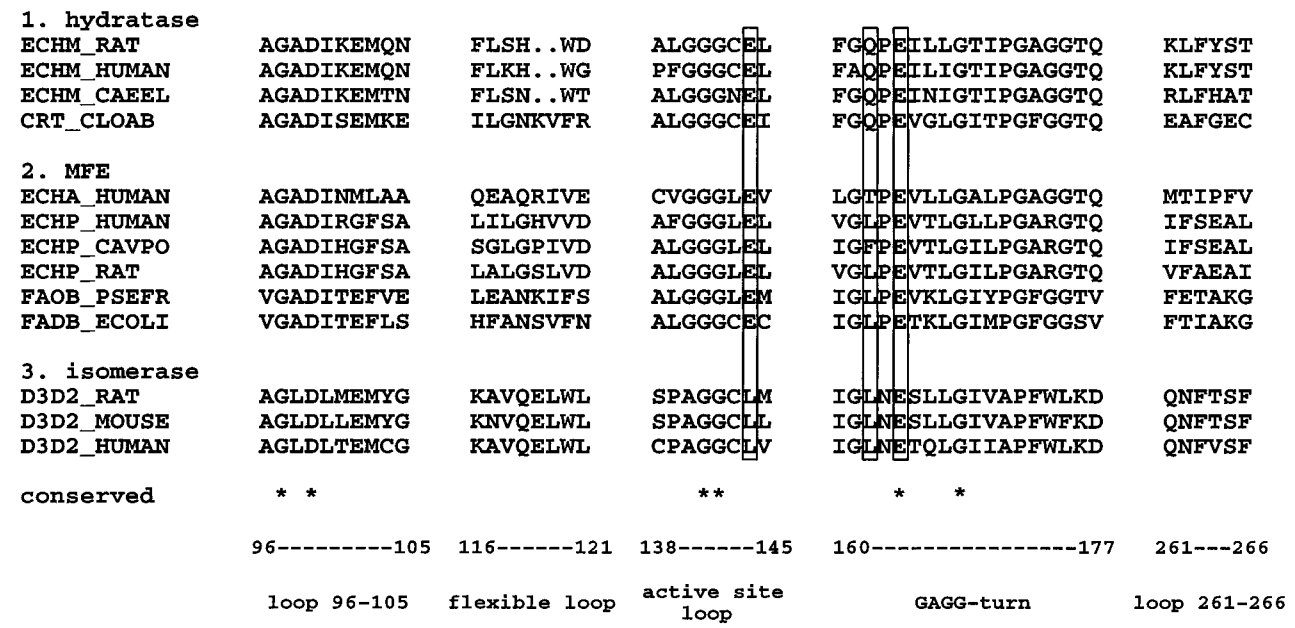

FIGURE 3: Sequence conservation within members of the sequence families catalyzing hydratase or isomerase reactions for residues close to the active site (Figure 2). The numbering scheme corresponds to the mECH-1 sequence (ECHM_RAT). The sequence identifiers specify the Swissprot entry code (*42*). The completely conserved residues are highlighted on the consensus line. Main chain atoms of the loop 96−105 interact with the adenine ring of the CoA moiety and with the carbonyl oxygen of the fatty acid. Residues of the flexible loop become disordered when binding octanoyl-CoA (*22*). The residues of the active site helix are part of the hydratase/isomerase sequence fingerprint. The main chain nitrogen atoms of the GAGG turn form hydrogen bonds to the catalytic glutamate Glu144 and to the water molecule in the unliganded active site. Residue Phe263 points into the active site of an adjacent subunit. The residues corresponding to Glu144, Gln162, and Glu164 in ECHM_RAT are marked with a box.

sensitivity 20 mdeg, speed 50 nm/min, average of 40 scans, and path length 2 mm. The protein concentration was 12 μM. Near-UV spectra were measured from 250 to 330 nm in 200 mM KP_i and 3 mM EDTA, pH 7.2, buffer with the following instrument settings: response 1 s, sensitivity 5 mdeg, speed 50 nm/min, average of 60 scans, and path length 10 mm. The protein concentration was 1.6 μM. The data were processed by subtracting the buffer spectrum and calculating molar ellipticity per residue.

Determination of K_m and k_{cat} Values for Enoyl-CoA Hydratase-1 Activity. The kinetic constants for the hydratase-1 activity were determined toward hydration of *trans*-2-hexenoyl-CoA and *trans*-2-decenoyl-CoA substrates by monitoring the subsequent oxidation of (*S*)-3-hydroxyacyl-CoA as a formation of the Mg^{2+} complex of 3-ketoacyl-CoA at 303 nm. Reaction buffer consisted of 50 mM Tris-HCl and 50 mM KCl, pH 8.0, containing 1 mM NAD^+ (E. Merck, Darmstadt, Germany), 1 mM sodium pyruvate (Sigma Chemicals), and 2.5 mM $MgCl_2$. The measurement was performed in a final volume of 0.5 mL at 22 °C. The mixture also contained 3.4 units of (*S*)-3-hydroxyacyl-CoA dehydrogenase (Sigma Chemicals) and 21 units of L-lactic dehydrogenase (Sigma Chemicals) as auxiliary enzymes. The substrate concentrations for *trans*-2-decenoyl-CoA were 1, 5, 10, 20, 30, 40, and 60 μM and for *trans*-2-hexenoyl-CoA 10, 20, 30, 40, 50, 60, 80, and 100 μM.

Δ^3-Δ^2-Enoyl-CoA Isomerase Activity of mECH-1. To study whether mECH-1 catalyzes Δ^3-Δ^2 isomerization, 0.13 μmol of *trans*-3-hexenoyl-CoA in 20 μL of 200 mM KP_i buffer, pH 7.4, was incubated with 2 μg of recombinant mECH-1 in 10 μL of a solution containing 200 mM KP_i, 3 mM EDTA, and 3 mM EGTA, pH 7.4 at 37 °C. As a blank, 2 μg of recombinant mECH-1 was heated to 95 °C for 15 min before addition of the substrate.

After the incubations, 30 μL of acetone was added to the reaction mixtures, and the solutions were taken to dryness under a stream of nitrogen at 30 °C. After addition of 10 μL of 5 mM 2-methylvaleric acid (Aldrich Chemie, Steinheim, Germany) in ethanol as an internal standard and 25 μL of 1 M HCl in ethanol, the samples were mixed, shortly treated with ultrasound, and incubated overnight at 22 °C. After addition of 10 μL of 5 mM 1-decanol (Aldrich Chemie) in hexane as a second internal standard, the mixture was extracted three times with 100 μL of hexane each. The combined hexane phases were evaporated under a stream of nitrogen at 0 °C to a volume of about 20 μL.

Analysis was performed with a Hewlett-Packard gas chromatograph, type 5890 (Bad Homburg, Germany), equipped with a flame ionization detector and the GLC−column FS−OV-1701 (10 m × 0.32 mm), (CS-Chromatographie Service GmbH, Langerwehe, Germany) using the following temperature program: 3 min at 50 °C, 50−80 °C with 2 °C/min, 5 min at 80 °C, 80−220 °C with 20 °C/min, and 5 min at 220 °C. N_2 was used as a carrier gas, and the column head pressure was 50 kPa.

The observed intrinsic isomerase activity of mECH-1 was measured by modifying the isomerase assay (*14*) using 1.3 μg of recombinant 2-enoyl-CoA hydratase-2 from rat (*27*) and 0.5 μg of recombinant *R*-specific 3-hydroxyacyl-CoA dehydrogenase from yeast (*28*) as auxiliary enzymes. This allowed the measurement of formed *trans*-2-enoyl-CoA directly and independently of the hydratase-1. The substrate concentrations were for Glu144Ala, Gln162Ala, Gln162Leu, and Gln162Met 10, 20, 40, 60, 100, and 200 μM and for Glu164Ala and Glu144Ala,Gln162Leu only 60 μM. The kinetic data were analyzed by using GraFit computer software (Sigma Chemicals) with simple weighting.

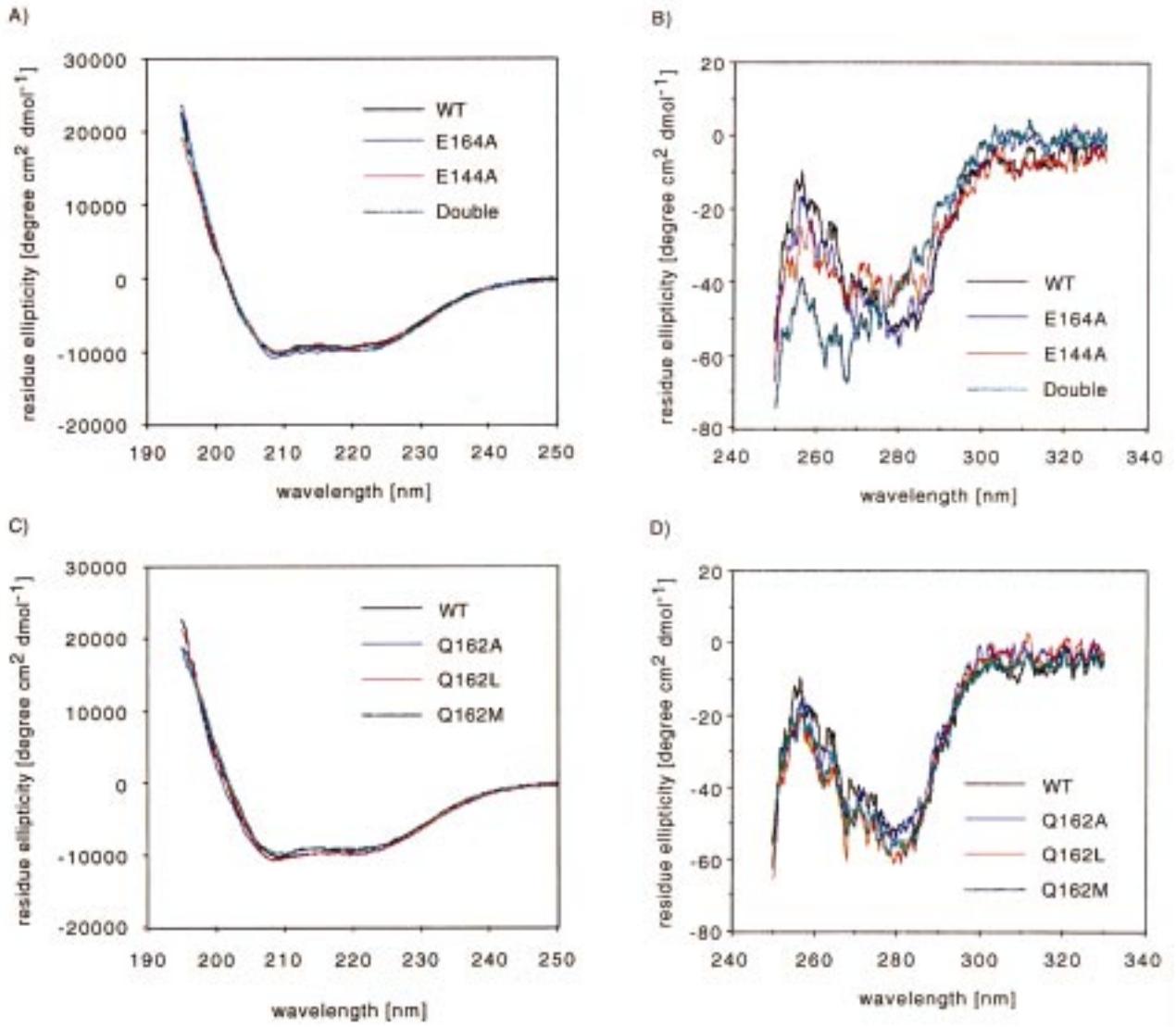

FIGURE 4: CD spectroscopy of recombinant 2-enoyl-CoA hydratase-1 and its variants. Far-UV spectra (A) and near-UV spectra (B) of active site residue mutants: black line, wild type; purple line, Glu164Ala; red line, Glu144Ala; green line, Glu144Ala,Gln162Leu (double). Far-UV CD spectra (C) and near-UV spectra (D) of Gln162 mutants: black line, wild type; purple line, Gln162Ala; red line, Gln162Leu; green line, Gln162Met.

Determination of the pH Dependence of the Hydratase and Isomerase Reaction. The kinetic parameters were determined at eight different pH values. The measurements were done in 200 mM KP_i buffers, and the pH of the buffers (ranging from 5.1 to 10.4) was checked just before the assays. For the hydratase reaction *trans*-2-hexenoyl-CoA was used as a substrate at concentrations of 20, 40, 60, and 100 μM at 22 °C. To determine the kinetic constants for isomerization, the isomerase activity was measured as given above using *trans*-3-hexenoyl-CoA as a substrate at concentrations of 20, 40, 60, and 100 μM. The kinetic data were transformed to Lineweaver−Burk plots by using GraFit computer software. The K_m values at different pH values were calculated from the slopes of the curves and the catalytic turnover numbers by dividing the maximal velocities at different pH values with the total enzyme amount in the reaction. The pH dependence curves of the k_{cat}/K_m for hydratase and isomerase reactions, the pK_a values, and their errors were calculated with the GraFit computer software.

Others. Protein concentrations were measured with Bio-Rad protein assay reagent (Bio-Rad Laboratories, Hercules, CA), and the protein samples were analyzed on 12% SDS−polyacrylamide gel. *trans*-2- and *trans*-3-hexenoic acids were from Aldrich Chemie and Lancaster Synthesis (Lancashire, UK), respectively. 3-Hydroxyhexanoic acid ethyl ester was synthesized by $NaBH_4$ reduction of 3-ketohexanoic acid ethyl ester (Aldrich Chemie). Acyl-CoA thioesters were prepared by the mixed anhydride method (*29*) and purified on reverse-phase silica gel (RP-18; ICN Chemicals, Costa Mesa, CA) or on a μBondapak C_{18} column (Waters, Milford, MA). The substrates were verified by determining their mass with a MALDI-TOF mass spectrometer (Kompact MALDI III, Kratos Analytical, Manchester, U.K.) and by testing them as biological substrates with proper enzymes.

RESULTS AND DISCUSSION

Overexpression and Purification of Recombinant Wild-Type and Mutated Versions of mECH-1. The overexpressed recombinant mECH-1 from the pET3aECH1 vector in *E. coli* BL21(DE3)pLysS contained the initiation methionine followed by the mature form of mECH-1, starting at amino acid Gly30 [the 29 amino acids of the mitochondrial targeting

Table 1: Kinetic Constants of the Hydratase Activity and the Isomerase Activity of Recombinant Wild-Type and Mutant mECH-1 for *trans*-2-Hexenoyl-CoA, *trans*-2-Decenoyl-CoA, and *trans*-3-Hexenoyl-CoA

	hydratase				isomerase	
	trans-2-hexenoyl-CoA		*trans*-2-decenoyl-CoA		*trans*-3-hexenoyl-CoA	
	K_m (μM)	k_{cat} (s^{-1})	K_m (μM)	k_{cat} (s^{-1})	K_m (μM)	k_{cat} (s^{-1})
mECH-1	25.0 ± 2.9	745 ± 30	4.9 ± 1.2	203 ± 10	65.5 ± 16.0	0.127 ± 0.009
Glu144Ala	15.2 ± 2.1	0.430 ± 0.016	3.0 ± 0.5	0.085 ± 0.002	230 ± 66	0.013 ± 0.002
Glu164Ala	23.5 ± 6.1	0.436 ± 0.050	5.2 ± 2.1	0.095 ± 0.009	nd	0.0001[a]
Gln162Leu	27.0 ± 8.6	561 ± 64	5.0 ± 0.7	174 ± 6	74.7 ± 24.6	0.041 ± 0.006
Gln162Met	22.9 ± 4.4	601 ± 38	6.3 ± 0.8	164 ± 5	59.3 ± 7.4	0.030 ± 0.002
Gln162Ala	14.3 ± 2.7	607 ± 30	2.9 ± 0.6	104 ± 4	41.7 ± 8.2	0.039 ± 0.003
Glu144Ala,Gln162Leu	21.0 ± 2.3	0.060 ± 0.002	2.5 ± 0.4	0.0121 ± 0.0003	nd	0.00006[a]

[a] Calculated from the maximal velocity measured using 60 μM substrate concentration with high concentration of the mutant protein. The K_m value could not be determined (nd).

signal (*30*) are omitted]. The 2-enoyl-CoA hydratase-1 activity was 64 μmol min^{-1} (mg of protein)$^{-1}$ in the homogenate of cells transformed with the pET3aECH1 expression vector versus 0.02 μmol min^{-1} (mg of protein)$^{-1}$ in the homogenate of cells transformed with the vector only. The recombinant mECH-1 and its mutated variants were purified from the soluble fraction of the *E. coli* cell lysate as described under Materials and Methods. The SDS−PAGE analysis revealed only one band with a molecular mass of 28 kDa. In size-exclusion chromatography the retention volumes of the recombinant hydratase proteins were the same as that of the wild-type enzyme purified from rat liver. This result indicated that the proteins obtained by this procedure are hexamers like the wild-type protein, in contrast to earlier studies (*20*) where a trimer was obtained when mECH-1 was expressed as a recombinant protein.

Spectroscopic Studies on Recombinant mECH-1 and Its Variants. To investigate the folding of the various recombinant mECH-1 variants, CD spectra in the far-UV region (195−250 nm) were measured. The observed spectra of rat liver wild type and recombinant wild type were practically the same (data not shown). As shown in Figure 4A,C the far-UV spectra for the mutated variants and the recombinant wild type are also the same, indicating that the mutations do not cause a change in the composition of secondary structure elements. Thus, the data are in line with the size-exclusion chromatography, verifying that the recombinant mECH-1 proteins are properly folded and assembled.

In the near-UV region (250−350 nm) the single mutants and the wild type have practically identical spectra (Figure 4B,D). The double mutant (Glu144Ala,Gln162Leu), however, shows a change of ellipticity (Figure 4B) in the 255−280 nm region, suggesting local structural changes (see below).

Hydratase Activity of Recombinant mECH-1 and Its Glu144Ala and Glu164Ala Variants. When the enzymatic properties of wild-type recombinant mECH-1 were measured using crotonyl-CoA as a substrate, a K_m of 49.9 ± 6.3 μM and a k_{cat} of 2238 ± 124 s^{-1} were obtained. These values are in accordance with the earlier published data [K_m of 40 μM, k_{cat} of 2150 s^{-1} (*31*), K_m of 70 μM, k_{cat} of 3500 s^{-1} (*20*)]. The K_m and the k_{cat} values for the C6 and C10 substrates are listed in Table 1.

The Glu164Ala variant had a 2000 times lower catalytic activity than the wild-type recombinant mECH-1 with the C6 and C10 substrates, but the K_m values were unchanged (Table 1). The observed decrease in the catalytic activity is significantly less than the value reported earlier for a Glu164Gln variant of mECH-1 (*20*), having the catalytic activity about 100 000-fold decreased. However, the K_m value (for crotonyl-CoA as substrate) of the Glu164Gln variant was only moderately affected (*20*), similar to that observed for the Glu164Ala variant reported in this investigation (Table 1). The difference in the decrease of k_{cat} values between the Glu164Ala variants might come from the fact that in the Glu164Ala mutant a water molecule could occupy the space of the removed Glu164 side chain, thereby facilitating catalysis. In the Glu164Gln mutant the glutamine side chain replaces the glutamate side chain, which could exclude the presence of an additional water molecule.

When the carboxylic side chain of Glu144, which activates the active site water molecule (Figures 2 and 3), was replaced by a methyl group (Glu144Ala), the catalytic activity decreased 2000 times (similar to the rate decrease seen for the Glu164Ala variant) without any major change in the K_m value. Because both Glu164Ala and Glu144Ala showed a highly decreased catalytic activity but at the same time the protein folding pattern was unchanged (CD spectroscopy and size-exclusion chromatography), the data confirm that Glu144 and Glu164 act as protic amino acid residues participating in the catalysis.

Isomerase Activity of Recombinant mECH-1 and Its Glu144Ala and Glu164Ala Variants. Closely related to the hydratase reaction is the Δ^3-Δ^2 isomerization of enoyl-CoA substrates (Figure 1). The mitochondrial Δ^3-Δ^2-enoyl-CoA isomerase is sequence related to mECH-1 (*4*), and as discussed above the equivalent residue of Glu164 presumably carries out the same chemical reaction, which is the proton transfer of the α-carbon of the enoyl-CoA substrate (*20*). In this context it was relevant to investigate the possible isomerization reaction catalyzed by the wild type and mutated variants of the mECH-1.

mECH-1 was incubated with *trans*-3-hexenoyl-CoA over variable periods of time, and the incubation mixtures were analyzed for metabolites (Figure 5). After derivatization of the metabolites to the corresponding ethyl esters, GLC analysis showed accumulations of 2-hexenoic acid ethyl ester and 3-hydroxyhexanoic acid ethyl ester in a time-dependent manner. When *trans*-3-hexenoyl-CoA was incubated with heat-inactivated mECH-1, no formation of metabolites was observed (Figure 5). These data were interpreted to show that in the presence of mECH-1 *trans*-3-hexenoyl-CoA was first isomerized to 2-hexenoyl-CoA, which was subsequently hydrated to 3-hydroxyhexanoyl-CoA.

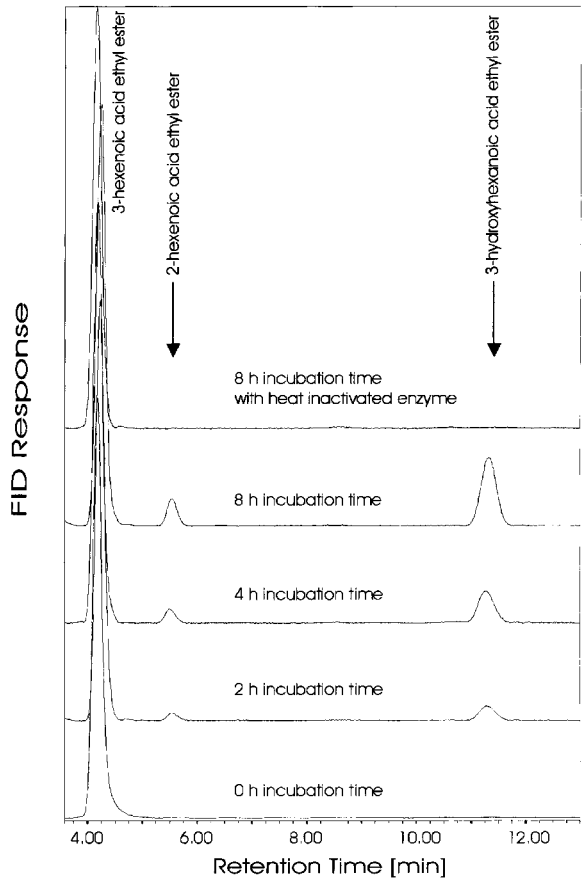

FIGURE 5: GLC analysis of metabolites from *trans*-3-hexenoyl-CoA incubated with mECH-1. After incubation of *trans*-3-hexenoyl-CoA with mECH-1 for the indicated period of time, the metabolites were derivatized to the corresponding ethyl esters and analyzed by a GLC as described under Materials and Methods. The retention times for *trans*-3-hexenoic acid ethyl ester, *trans*-2-hexenoic acid ethyl ester, and 3-hydroxyhexanoic acid ethyl ester under the assay conditions were determined separately with standard compounds and are indicated by arrows in the figure. The *Y*-axis shows the relative response of the flame ionization detector (FID).

Because of the limited sensitivity of the GLC detection for kinetic analysis of the isomerization by mECH-1, a spectrophotometric assay method was developed on the basis of the production of NADH. The product of isomerization, *trans*-2-hexenoyl-CoA, was hydrated to (*R*)-3-hydroxyhexanoyl-CoA by recombinant 2-enoyl-CoA hydratase-2. The generated (*R*)-3-hydroxyhexanoyl-CoA was oxidized to 3-ketohexanoyl-CoA by recombinant yeast (*R*)-3-hydroxyacyl-CoA dehydrogenase in the presence of NAD^+. Control incubation of auxiliary enzymes (2-enoyl-CoA hydratase-2 and *R*-specific 3-hydroxyacyl-CoA dehydrogenase) with *trans*-3-hexenoyl-CoA did not give any reactions. This observation agrees with the notion that 2-enoyl-CoA hydratase-2 (*27*) or the peroxisomal MFE type 2 from either mammals (*32*) or yeast (*28*) does not catalyze isomerase reaction. In addition to the GLC analysis of *trans*-3-hexenoyl-CoA metabolism (Figure 5), this finding also demonstrated that there was no detectable nonenzymatic isomerization. It is also worth pointing out that the mECH-1 protein used in this study was overexpressed in *E. coli* and isomerase from *E. coli* is known to be integral activity of the high molecular mass multifunctional β-oxidation enzyme having also 2-enoyl-CoA hydratase-1, 3-hydroxyacyl-CoA dehydrogenase, and 3-hydroxyacyl-CoA epimerase activities in the large α-subunit and 3-ketoacyl-CoA thiolase activity in the small β-subunit (*33*). When *trans*-3-hexenoyl-CoA was incubated with the mECH-1 preparation purified from *E. coli* lysate in the presence of NAD^+ but without added auxiliary enzymes, neither generation of NADH nor formation of 3-ketoacyl-CoA (monitored as the Mg^{2+}−3-ketoacyl-CoA complex) was observed. These findings rule out the possibility that the metabolites of *trans*-3-hexenoyl-CoA detected in the GLC analysis arose due to contaminating MFE of *E. coli* in the mECH-1 preparation.

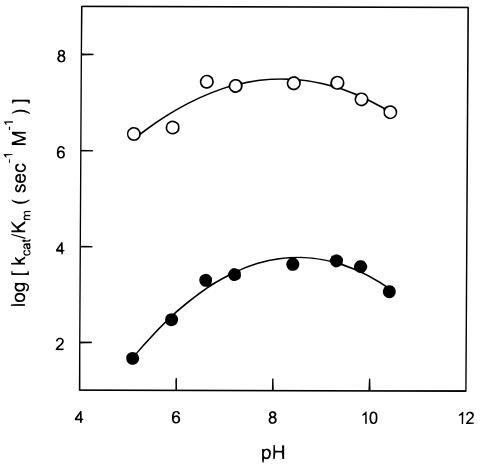

FIGURE 6: pH dependence of k_{cat}/K_m values for wild-type mECH-1. The pH dependencies of the hydratase reaction (○) (using *trans*-2-hexenoyl-CoA as a substrate) and the isomerase reaction (●) (using *trans*-3-hexenoyl-CoA as a substrate) are shown. Curves were fitted with the GraFit computer program.

When the enzymatic isomerase assay was applied, recombinant mECH-1 was found to catalyze isomerization with the rate of $^1/_{5000}$ of the hydration rate (C6 substrates, Table 1). The isomerization activity of hydratase (k_{cat} of 0.127 s^{-1}, Table 1) is about 150-fold lower than the activity of the monofunctional mitochondrial Δ^3-Δ^2-enoyl-CoA isomerase [k_{cat} of 19.2 s^{-1} (*34*)] for the same substrate. The isomerase activity of mECH-1 is interesting in view of the fact that both activities can be found in the N-terminal modules of peroxisomal MFE type 1 from rat (*14*) and the large subunit of *E. coli* MFE (*35*). On the basis of inhibitor studies it was suggested that both reactions take place in the same active site (*15*), and our observation of the residual isomerase activity by the hydratase supports this hypothesis. In the Glu164Ala variant the isomerase activity was decreased 1000-fold, whereas in the Glu144Ala variant it was decreased only about 10-fold. These results show that Glu164 is crucial for the hydratase and the isomerase reactions of mECH-1, but the question remains as to which structural features determine their relative rates.

pH Dependence of k_{cat}/K_m for Hydratase and Isomerase Reactions Catalyzed by mECH-1. The pH dependence curve of k_{cat}/K_m for the wild-type hydratase reaction (measured in the direction of hydration) is bell-shaped (Figure 6) with an estimated pK_{a1} of 6.6 ± 0.2 and pK_{a2} of 9.9 ± 0.1. The shape of the curve was similar to that determined for the hydratase reaction of *E. coli* MFE (*19*). In *E. coli* MFE the corresponding pK_a values have been assigned to Glu119 and Glu139, which are equivalent to Glu144 and Glu164 in mECH-1. In line with this, the mutational data (Table 1) and structural data (*3*, *22*) indicate the importance of Glu144

and Glu164 for the catalysis. Consequently, the pK_{a1} probably concerns the Glu144 and the pK_{a2} attributes to Glu164 (base B_2^- and acid B_1, respectively, in Figure 1A). The isomerase reaction requires at least two proton transfers, and indeed, the profile of the pH dependence curve of k_{cat}/K_m for isomerization is also bell-shaped (Figure 6) with an estimated pK_{a1} of 7.1 ± 0.1 and pK_{a2} of 10.1 ± 0.2. The site-directed mutagenesis and sequence alignments of known isomerases and hydratases suggest that Glu164 is one of the protic residues involved in the catalysis (corresponding to B_a^- in Figure 1B). In the pH dependence curve (Figure 6) of k_{cat}/K_m (for conversion of *trans*-3-enoyl-CoA into *trans*-2-enoyl-CoA) pK_{a1} (associated with B_a^- in Figure 1B) probably corresponds to Glu164 and pK_{a2} is associated with the unknown proton donor function (B_b in Figure 1B). In the complex of mECH-1 and acetoacetyl-CoA, the distances of the C2 and C4 atoms of acetoacetyl-CoA to the nearest carboxylate oxygen atom of Glu164 are 3.7 and 4.5 Å, respectively; therefore if this glutamate functions as the unknown protic residue B_b, it would need to have conformational flexibility in order to be able to shuttle the proton between the 2 and 4 position of the 3-enoyl-CoA substrate in the isomerase reaction.

Importance of Gln162 for the Rate of the Hydratase and Isomerase Reaction. The analysis of the active site architecture in the solved mECH-1 structure shows that the side chain of the catalytic Glu164 is fixed to the side chain of Gln162 by two hydrogen bonds (Figure 2). This anchoring interaction could interfere with the postulated shuttling of protons by the Glu164 side chain in the isomerase reaction. Sequence alignment of members of the hydratase/isomerase protein family (Figure 3) shows that position 162 is occupied by a leucine in the monofunctional isomerases and in most of the MFEs, but it is a conserved glutamine in the hydratases. To study whether the fixation of Glu164 (by Gln162) favors the hydratase reaction over the isomerase reaction, Gln162 was mutated to leucine, methionine, and alanine. The mutated variants had almost the same catalytic properties concerning the hydratase reaction; the k_{cat} values were only moderately decreased, but the K_m values remained unchanged. For the isomerase reaction the k_{cat} decreased by a factor of 3 while the K_m did not change. The result is similar if Gln162 is replaced with a methionine (roughly the same size as a glutamine) or an alanine (a small and neutral amino acid residue). Therefore, the properties of these variants indicate that Gln162 is not important for favoring the hydratase over the isomerase reaction, suggesting that Glu164 is not involved in proton shuttling between the 2 and 4 position in the isomerase reaction. These results are consistent with the notion that the active site water molecule is important for proton exchange at the C4 atom in the isomerase reaction.

Properties of the Glu144Ala,Gln162Leu Variant. The enzymological characterization of the Glu144Ala,Gln162Leu mutant provides some further insight into the active site properties. It is found (Table 1) that for this double mutant the catalytic turnover rate of the hydration drops to a value about 10-fold lower than for the single mutant Glu144Ala alone, whereas the isomerization rate of the double mutant (Glu144Ala,Gln162Leu) even drops to a value 200-fold lower than the rate of the Glu144Ala mutant. The catalytic rates of the double mutant are very low. The double mutant is also the only variant with changes in the near-UV spectra (Figure 4). These changes suggest structural differences between the wild type and this variant. The near-UV spectra are dominated by tryptophans. In mECH-1 there is only one tryptophan, Trp120, which is in the flexible loop (*3*, *22*) forming one part of the substrate binding pocket near the active site helix. As can be seen in Figure 2, Trp120 is in van der Waals contact with residues Gly141 (shortest distance is 3.4 Å) and Glu144 (shortest distance is 4.3 Å) of this helix. This tryptophan is known to become disordered in the presence of octanoyl-CoA, due to the presence of the C8 fatty acid tail (*22*). The spectroscopic data suggest that in the double mutant this tryptophan is also in a different environment, even in the absence of a ligand. This change in structure is only observed in the double mutant (Glu144Ala,-Gln162Leu) and not in the individual mutants. Apparently the synergism of the two mutations causes this change in structure. Inspection of the active site geometry (Figure 2) shows that Glu144, which is in the middle of the active site helix, is hydrogen bonded to Gln162 and to the GAGG loop as well as to the active site water. Gln162 is anchored to Glu164 but also to several residues of the active site helix via hydrogen bonds to main chain atoms and side chain atoms of Gly140, Cys143, and Glu144 (Figure 2). Therefore, the conformation of the active site helix (residues 141−148) is stabilized by hydrogen-bonding interactions of both Glu144 and Gln162. The point mutations Glu144Ala and Gln162Leu by themselves apparently do not cause structural rearrangements of the active site helix, but when both residues are changed, the active site geometry changes. This would force Trp120 to adopt another conformation, causing the change in the near-UV spectrum (Figure 4), and this would also explain the almost complete absence of catalytic activity of this double mutant (Table 1).

CONCLUDING REMARKS

These enzymological studies have shown that the active site of mECH-1 can also catalyze the isomerase reaction. The isomerase activity of the Glu164Ala variant is very low, while for the Glu144Ala variant the decrease of the rate of isomerization is much less. If Glu164 is the only essential catalytic residue for the isomerization reaction, then it remains to be understood why the isomerase rate is 5000-fold lower than the hydratase rate, whereas the active site of MFE type 1 can catalyze these two reactions with more similar rates. For example, in rat peroxisomal MFE type 1 the hydratase rate (measured with *trans*-2-decenoyl-CoA as a substrate) is only 10 times higher than the isomerase rate (measured with *trans*-3-decenoyl-CoA as a substrate) (*14*). The mutagenesis and kinetic data of mECH-1 indicate that the anchoring interactions between the side chains of Gln162 and Glu164 are not important for favoring the hydratase over the isomerase reaction. Another important factor determining the rate of isomerization will be the conformation of the bound fatty acid tail (*36*, *37*) and the active site electric potential (*18*, *38*). Therefore, the relative rates of the hydratase and isomerase reactions will not only be determined by the presence of the catalytic residues as such but will also be influenced by the shape and charge distribution of the active site pocket. It is therefore predicted that these active site properties of peroxisomal MFE type 1 or isomerase will be different from hydratase.

ACKNOWLEDGMENT

We thank Tanja Kokko and Marika Yppärilä for their technical assistance, Anna-Leena Hietajärvi for substrate synthesis, and Yorgo Modis for preparing Figure 2A. The (*R*)-specific 3-hydroxyacyl-CoA dehydrogenase was a kind gift from Antti Haapalainen, Biocenter Oulu, University of Oulu.

REFERENCES

1. Stern, J. R., Del Campillo, A., and Raw, J. (1953) *J. Am. Chem. Soc. 75*, 2277−2278.
2. Waterson, R. M., and Hill, R. L. (1972) *J. Biol. Chem. 247*, 5258−5265.
3. Engel, C. K., Mathieu, M., Zeelen, J. Ph., Hiltunen, J. K., and Wierenga, R. K. (1996) *EMBO J. 15*, 5135−5145.
4. Palosaari, P. M., Vihinen, M., Mäntsälä, P. I., Alexson, S. E. H., Pihlajaniemi, T., and Hiltunen, J. K. (1991) *J. Biol. Chem. 266*, 10750−10753.
5. Müller-Newen, G., and Stoffel, W. (1991) *Biol. Chem. Hoppe-Seyler 372*, 613−624.
6. Babbitt, P. C., Kenyon, G. L., Martin, B. M., Charest, H., Slyvestre, M., Scholten, J. D., Chang, K.-H., Liang, P.-H., and Dunaway-Mariano, D. (1992) *Biochemistry 31*, 5594−5604.
7. Schmitz, A., Gartemann, K. H., Fiedler, J., Grund, E., and Eichenlaub, R. (1992) *Appl. Environ. Microbiol. 58*, 4068−4071.
8. Osumi, T., Ishii, N., Hijikata, M., Kamijo, K., Ozasa, H., Furuta, S., Miyazawa, S., Kondo, K., Inoue, K., Kagamiyama, H., and Hashimoto, T. (1985) *J. Biol. Chem. 260*, 8905−8910.
9. DiRusso, C. C. (1990) *J. Bacteriol. 172*, 6459−6468.
10. Uchida, Y., Izai, K., Orii, T., and Hashimoto, T. (1992) *J. Biol. Chem. 267*, 1034−1041.
11. Filppula, S. A., Yagi, A. I., Kilpeläinen, S. H., Novikov, D., FitzPatrick, D. R., Vihinen, M., Valle, D., and Hiltunen, J. K. (1998) *J. Biol. Chem. 273*, 349−355.
12. Driscoll, J. R., and Taber, H. W. (1992) *J. Bacteriol. 174*, 5063−5071.
13. Eichler, K., Bourgis, F., Buchet, A., Kleber, H. P., and Mandrand-Berthelot, M. A. (1994) *Mol. Microbiol. 13*, 775−786.
14. Palosaari, P. M., and Hiltunen, J. K. (1990) *J. Biol. Chem. 265*, 2446−2449.
15. Yang, S.-Y., He, X.-Y., and Schulz, H. (1995) *Biochemistry 34*, 6441−6447.
16. Willadsen, P., and Eggerer, H. (1975) *Eur. J. Biochem. 54*, 247−252.
17. Bahnson, B. J., and Anderson, V. E. (1991) *Biochemistry 30*, 5894−5906.
18. Wu, W.-J., Anderson, V. E., Raleigh, D. P., and Tonge, P. J. (1997) *Biochemistry 36*, 2211−2220.
19. He, X.-Y., and Yang, S.-Y. (1997) *Biochemistry 36*, 11044−11049.
20. Müller-Newen, G., Janssen, U., and Stoffel, W. (1995) *Eur. J. Biochem. 228*, 68−73.
21. D'Ordine, R. L., Bahnson, B. J., Tonge, P. J., and Anderson, V. E. (1994) *Biochemistry 33*, 14733−14742.
22. Engel, C. K., Kiema, T. R., Hiltunen, J. K., and Wierenga, R. K. (1998) *J. Mol. Biol. 275*, 847−859.
23. Müller-Newen, G., and Stoffel, W. (1993) *Biochemistry 32*, 11405−11412.
24. Zeelen, J. P., Pauptit, R. A., Wierenga, R. K., Kunau, W. H., and Hiltunen, J. K. (1992) *J. Mol. Biol. 224*, 273−275.
25. Ho, S. N., Hunt, H. D., Horton, R. M., Pullen, J. K., and Pease, L. R. (1989) *Gene 77*, 51−59.
26. Pace, C. N., Vajdos, F., Fee, L., Grimsley, G., and Gray, T. (1995) *Protein Sci. 4*, 2411−2423.
27. Qin, Y.-M., Haapalainen, A. M., Conry, D., Cuebas, D. A., Hiltunen, J. K., and Novikov, D. K. (1997) *Biochem. J. 328*, 377−382.
28. Hiltunen, J. K., Wenzel, B., Beyer, A., Erdmann, R., Fosså, A., and Kunau, W.-H. (1992) *J. Biol. Chem. 267*, 6646−6653.
29. Rasmussen, J. T., Börchers, T., and Knudsen, J. (1991) *Biochem. J. 265*, 849−855.
30. Minami-Ishii, N., Taketani, S., Osumi, T., and Hasimoto, T. (1989) *Eur. J. Biochem. 185*, 73−78.
31. Furuta, S., Miyazawa, S., Osumi, T., Hashimoto, T., and Ui, N. (1980) *J. Biochem. 88*, 1059−1070.
32. Qin, Y.-M., Poutanen, M. H., Helander, H. M., Kvist, A.-P., Siivari, K. M., Schmitz, W., Conzelmann, E., Hellman U., and Hiltunen J. K. (1997) *Biochem. J. 321*, 21−28.
33. Yang, S. Y., and Schulz, H. (1983) *J. Biol. Chem. 258*, 9780−9785.
34. Palosaari, P. M., Kilponen, J. M., Sormunen, R. T., Hassinen, I. E., and Hiltunen, J. K. (1990) *J. Biol. Chem. 265*, 3347−3353.
35. Pramanik, A., Pawar, S., Antonian, E., and Schulz, H. (1979) *J. Bacteriol. 137*, 469−473.
36. Sacchettini, J. C., and Poulter, C. D. (1997) *Science 277*, 1788−1789.
37. Corey, E. J., and Sneen, R. A. (1956) *J. Am. Chem. Soc. 78*, 6269−6278.
38. D'Ordine, R. L., Tonge, P. J., Carey, P. R., and Anderson, V. E. (1994) *Biochemistry 33*, 12635−12643.
39. Kraulis, P. J. (1991) *J. Appl. Crystallogr. 24*, 946−950.
40. Merritt, E. A., and Bacon, D. J. (1997) *Methods Enzymol. 277*, 505−524.
41. Abagyan, R. A. (1998) *The ICM 2.6 Manual* (http://molsoft.com), Molsoft LCC, New York.
42. Bairoch, A., and Apweiler, R. (1998) *Nucleic Acids Res. 26*, 38−42.

BI981646V